

Spectroscopy of Single- and Double-Wall Carbon Nanotubes in Different Environments

Tobias Hertel,^{*,†,‡} Axel Hagen,[‡] Vadim Talalaev,[§] Katharina Arnold,^{||}
Frank Hennrich,^{||} Manfred Kappes,^{||} Sandra Rosenthal,[⊥] James McBride,[⊥]
Hendrik Ulbricht,[†] and Emmanuel Flahaut[#]

*Department of Physics and Astronomy, Vanderbilt University, Nashville, Tennessee,
Department of Physical Chemistry, Fritz-Haber-Institut der Max-Planck-Gesellschaft,
Berlin, Germany, Max-Born-Institute, Berlin, Germany Karlsruhe, Institut für
Nanotechnologie, Karlsruhe, Germany, Department of Chemistry, Vanderbilt
University, Nashville, Tennessee, and Forschungszentrum CIRIMAT/LCMIE,
UMR CNRS 5085, Université Paul Sabatier, Toulouse, France*

Received January 13, 2005; Revised Manuscript Received January 30, 2005

ABSTRACT

Individual single-wall carbon nanotubes (SWNTs) and double-wall carbon nanotubes (DWNTs) were suspended in water for optical studies using sodium-cholate and other surfactants. We used time-resolved photoluminescence (PL) spectroscopy to study the influence of tube chirality and diameter as well as of the environment on nonradiative decay in small diameter tubes. The studies provide evidence for PL from small diameter core tubes in DWNTs and for a correlation of nonradiative decay with tube diameter and exciton red shift as induced by interaction with the environment.

The optical properties of carbon nanotubes (CNTs) are studied increasingly for their potential in a variety of optical and optoelectronic applications.^{1–3} Light-emitting and photosensitive devices have already been fabricated and call for a more thorough investigation of fundamental optical processes and dynamics associated with optical excitations in CNTs. The photoluminescence-quantum yield (PL-QY) and branching ratios for optical excitations, for example, are of fundamental importance for the performance and potential of CNTs for optical devices. Here, the ability to control and tailor CNTs with specific optical properties will be crucial to facilitate their implementation in viable technologies.

However, apart from their alleged potential for applications, the geometrical and electronic structure of CNTs furnishes these one-dimensional macromolecules with unique optical properties that are also fascinating from a fundamental perspective.^{4,5} Optical properties and dynamics of excited states in CNTs are thus studied in growing detail with respect

to the competition of radiative with nonradiative decay processes, the influence of magnetic fields, and more.^{6–17}

Here, we explore optical excitations and the dynamics of optically excited single- and double-wall carbon nanotubes (SWNTs and DWNTs) in different environments. The results provide evidence for PL from cores of DWNTs as well as for a correlation of nonradiative decay rates with tube diameter and exciton red shift.

Double-wall carbon nanotubes were prepared by the technique developed by Flahaut and co-workers.¹⁸ A systematic analysis of TEM images such as the one shown in Figure 1A reveals that samples produced by this method contain approximately 77% of DWNTs—the high proportion of DWNTs was also confirmed by electron diffraction¹⁹—with a small admixture of about 18% single-wall carbon nanotubes (SWNTs), and roughly 5% triple-wall carbon nanotubes, see Figure 1B.¹⁹ Figure 1C shows the diameter distributions of core and shell tubes of DWNTs compared to the relative frequency of SWNTs. Important for the following discussion is that about 90% of the tubes with a diameter of below 1 nm are expected to be core tubes of DWNTs and that only about 10% of the small diameter tubes are residual SWNTs in the material. This assertion is justified by the observation that, to the best of our knowledge, no significant enrichment of tube concentrations by the process-

* Corresponding author. E-mail: Tobias.hertel@vanderbilt.edu; phone: +1 (615) 322-2864.

[†] Department of Physics and Astronomy, Vanderbilt University.

[‡] Fritz-Haber-Institut der Max-Planck-Gesellschaft.

[§] Max-Born-Institute.

^{||} Institut für Nanotechnologie.

[⊥] Department of Chemistry, Vanderbilt University.

[#] Université Paul Sabatier.

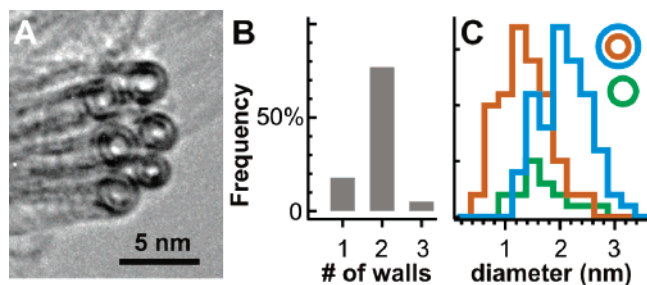


Figure 1. (A) TEM image of a DWNT sample. (B) Frequency of SWNTs, DWNTs, and TWNTs in raw soot. (C) Diameter distribution of core and shell tubes compared with the distribution of residual individual tubes in the suspensions used in these studies (adapted from ref 19).

ing techniques employed here has been reported previously. Preliminary TEM studies of suspended and centrifuged DWNTs likewise provide no evidence for enrichment of some sort. In the discussion of the time-resolved PL data we will concentrate on a few of the small diameter tubes.

SWNTs used here were obtained commercially from tubes@rice (laser vaporization process) or from Carbon Nanotechnologies Incorporated (HiPCO process). Suspensions of surfactant stabilized nanotubes were produced in the usual manner by ultrasonication of 1 wt % of surfactant in 10 mL H₂O or D₂O with 1 mg nanotube soot. The resulting suspensions were centrifuged with 50 000 g for 4 h before the supernatant was collected for spectroscopic investigation.²⁰

For time-resolved PL measurements, CNT suspensions were excited at 795 nm using 80 fs pulses from an 82 MHz Tsunami Ti:sapphire oscillator with an averaged output power of 300 mW. Pulse fluences were kept below 10¹³ photons per cm². PL was detected up to 1300 nm by a Hamamatsu streak camera with an IR-enhanced photocathode operating in synchroscan mode, whereas spectral selection is provided by an imaging-monochromator integrated into the detection system. The system response to nonresonantly scattered incident light is about 10 ps. Experimental details regarding the measurement of photoluminescence excitation (PLE) spectra can be found in ref 21.

The surfactants used here were sodium dodecyl sulfate (SDS), sodium dodecylbenzene sulfonate (SDBS), sodium cholate, and ammonium cholate. Both cholates were found to yield suspensions with absorption and emission spectra of superior quality, in terms of intensities, in particular for the DWNT material (see inset of Figure 2). Other surfactants appeared to lead to higher nonresonant background absorption, and spectral features could not be as well resolved. Nevertheless, cholate–DWNT spectra were also found to ride on a pronounced nonresonant background, significantly higher than that commonly found for SWNT HiPCO material, for example.

In Figure 2 we also compare background-corrected spectra from DWNT–Na–cholate suspensions with spectra from SDS and Na–cholate suspended HiPCO material as well as Na–cholate suspended PLV material (pulsed laser vaporization), all in D₂O. Due to the broad tube diameter distribution

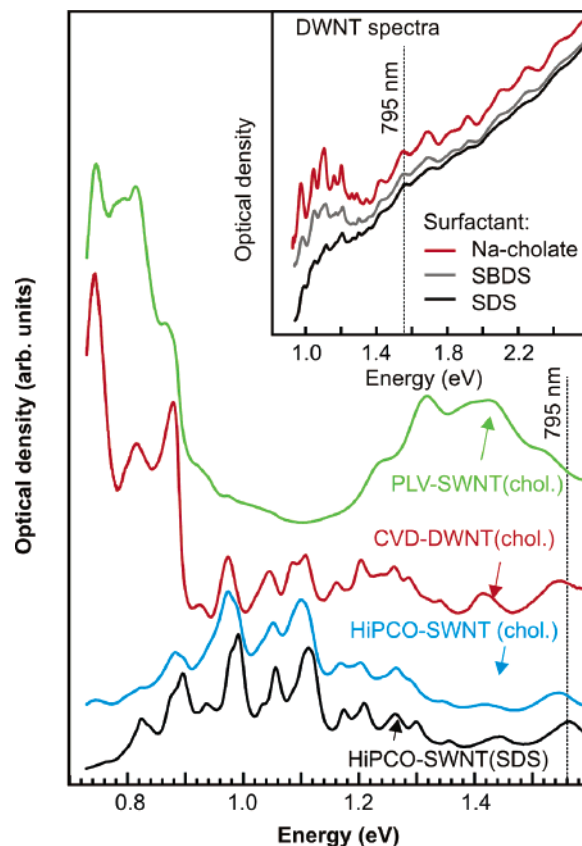


Figure 2. UV–VIS–NIR spectra of CNT–surfactant suspensions. The inset shows a comparison of sodium dodecyl sulfate, sodium dodecylbenzene sulfonate, and sodium cholate DWNT surfactant suspensions (in H₂O). Semiconducting E_{11} transitions for different systems in D₂O are seen in the background corrected absorption spectra in the lower part of the figure. Due to the broad distribution of diameters, spectra from the DWNT–cholate suspensions (red curves) bear resemblance with both spectra from larger diameter PLV and small diameter HiPCO material (green and blue/black curves, respectively). The dashed line indicates the excitation wavelength used for the time-resolved PL measurements.

of DWNT material and its maximum at a diameter of about 1.8 nm the corresponding absorption spectrum bears resemblance with both spectra from small diameter HiPCO as well as the larger diameter PLV–SWNT suspensions. Well-pronounced features in the energy range below about 1.4 eV can be attributed to excitonic E_{11} transitions associated with the first subbands of semiconducting CNTs. A comparison of the position of features from SWNT material dispersed in Na–cholate and in SDS reveals a 13 meV red shift in the cholate suspensions. By comparison, absorption features in the DWNT–cholate spectra are red-shifted by another 4 meV (see inset of Figure 4). Such shifts are here attributed to changes of the dielectric properties in the environment of the tubes.

An increase of the dielectric constant of the medium surrounding excited states, for example, allows for a better screening which will renormalize the binding energy of excitons as well as the optical free-carrier band-gap. Better screening will tend to reduce the exciton binding energy, but it will also reduce the free-carrier band-gap, two effects which partially compensate each other because the optical

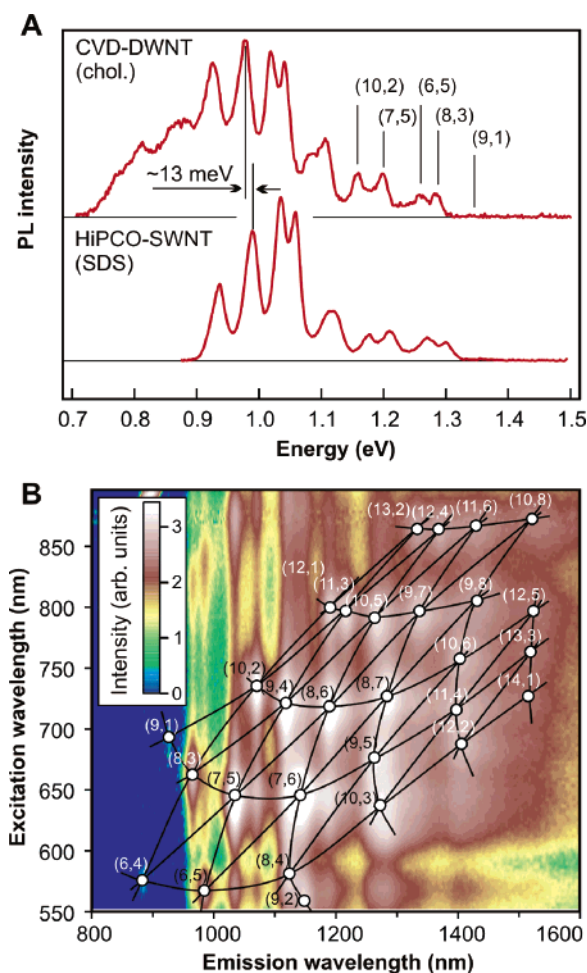


Figure 3. (A) PL spectra for excitation of DWNT–cholate and SWNT–SDS suspensions at 795 nm. (B) Photoluminescence excitation spectrum of a DWNT–cholate suspension. The labels indicate the specific tube types whose connectivity to other tube families is indicated by the solid black lines.

transition energy is given by the sum of both quantities. The overall trend, however, is expected to be that the change of the free-carrier gap outweighs changes in the exciton binding energy and consequently that an increase of dielectric screening leads to a decrease of the exciton transition energy.^{4,22} In the case of micelle suspended CNTs, we believe that the surrounding water plays an important role for the effective dielectric potential seen by the excitons. We speculate that the red shift and slight broadening of absorption features here observed for the cholate suspensions can be attributed to better access of water to the tube surface.

We also observe a red shift of E_{11} emission features in DWNT–Na–cholate PLE spectra relative to SWNT–SDS suspensions (see Figure 3). Interestingly, the average red shift of emission lines is 13 meV, while no appreciable change of energies is found for E_{22} transitions in absorption. One may speculate that this can be assigned to the frequency dependence of dielectric screening by the environment and the tube itself. Lower frequency contributions of the latter would then contribute to screening of “low frequency” E_{11} excited states but not of the high frequency E_{22} states. Note,

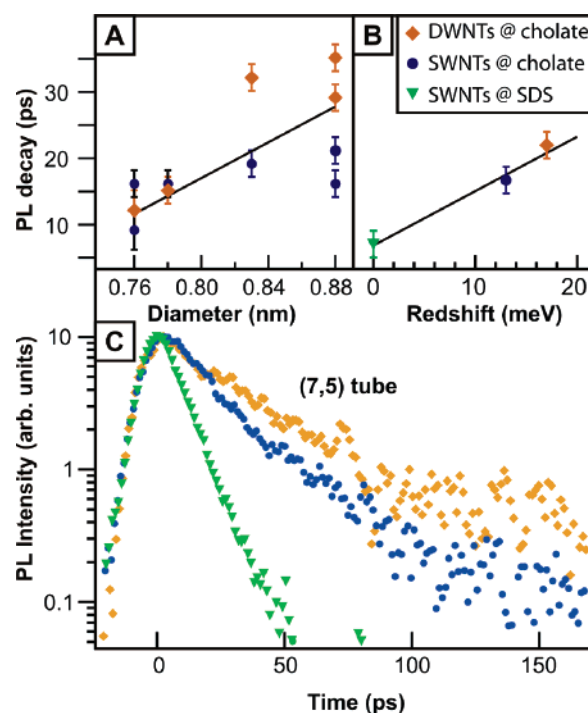


Figure 4. Comparison of PL decay from SWNTs and DWNT cores in different environments. (A) The PL decay times for 6 small diameter tubes reveal a weak correlation with the tube diameter. (B) The averaged decay time appears to correlate clearly with the redshift of absorption features. Solid lines in (A) and (B) are guides to the eye. (C) Comparison of the (7,5) PL signal in three different environments after excitation at 795 nm (diamonds, DWNT@cholate; circles, SWNT@cholate; triangles, SWNT–SDS).

that we find no evidence for spectral relaxation of E_{11} features within the instrumental response time of approximately 10 ps.

Additional information on dynamics of optically excited states and the competition between radiative and nonradiative decay in CNTs can be obtained from measured PL-QYs. A quantitative comparison of the optical densities associated with the spectra in Figure 1 shows that DWNT–cholate suspensions are typically about a factor of 2 optically less dense than their SWNT counterparts prepared under similar conditions. The PL signal from small diameter tubes on the other hand is about a factor of 2 higher, which implies that the effective QY of DWNT–cholate suspensions is roughly two to four times higher than that of SWNT–cholate or SWNT–SDS suspensions.

It remains to be clarified whether the PL signal from small diameter tubes in the DWNT samples has to be attributed to emission from majority or minority species, i.e., from DWNT cores or residual SWNTs. Two alternative, but similarly intriguing interpretations seem possible: (i) PL from small diameter tubes of DWNT suspensions is dominated by emission from core tubes where a moderate increase of the QY with respect to pure SWNT–cholate suspensions is evident from the above absorption and emission spectra, or (ii) the PL signal is dominated by residual SWNTs in these suspensions. To explain the high observed PL signals despite the low concentration of SWNTs in the latter case, one would

need to assume that the effective QY is over an order of magnitude higher than that of pure SWNT–cholate suspensions.

A measurement of the PL decay from small diameter tubes in DWNT suspensions, however, reveals that the PL decay times increase moderately by much less than an order of magnitude if DWNT–cholate suspensions are compared with SWNT–SDS suspensions. This can be associated with a modest increase of the PL quantum yield $\eta = \tau_{\text{PL}}/\tau_{\text{rad}}$ as determined by the change of radiative τ_{rad} and PL decay times τ_{PL} , where we assume that the radiative lifetime does not depend on the tube environment. We thus speculate that PL in the DWNT samples is dominated by core tubes of DWNTs and not by residual SWNTs. In the latter case one would expect over an order of magnitude increase of the PL decay time which is clearly not observed.

The decay of the PL signal for nonresonant excitation of the (7,5) tube at 795 nm is compared for different environments in Figure 4. In short, we observe two trends: (a) a correlation of the PL decay time with tube diameter (see Figure 4A) and (b) an overall increase of the PL decay time when going from SWNT–SDS over SWNT–cholate to DWNT–cholate suspensions, already discussed in the previous paragraph (see Figure 4B). The PL decay time from SWNT–SDS suspensions appears to be near or below the instrument response of about 10 ps. The PL decay in DWNT suspensions is thus found to be approximately three times longer if compared with SWNT–SDS suspensions. This is in agreement with the change of quantum yields estimated from absorption and emission spectra as discussed above and justified the above interpretation that PL from the DWNT suspensions is dominated by majority species, i.e., core tubes and not the minority SWNTs species. In the case of DWNT–cholate micelles, the slightly higher red shift if compared to the SWNT–cholate system may be associated with screening from shell tubes. This again supports the above interpretation that PL in DWNT samples is dominated by core tubes.

Somewhat surprisingly, the exciton red shift, i.e., better coupling of the exciton to the environment through screening leads to an increase of the PL decay time (see Figure 4B). This suggests that nonradiative decay does not directly occur by coupling to the environment but rather by some on-tube process such as trapping at specific sites, e.g., tube ends or defects. The increase of PL decay times with the red shift of emission features may indicate a reduction of the exciton mobility, for example.

The above conclusion that PL from DWNT suspensions is dominated by emission from core tubes also raises the question as to why PL from large band-gap core tubes is not efficiently quenched by resonant energy transfer to metallic or smaller gap semiconducting shell tubes. This implies that resonant excitation transfer between tubes of different chirality is slow with respect to the PL decay times

measured here. Such resonant tube-tube energy transfer might be suppressed by the incommensurability of the concentric core and shell tube unit cells. This suggests that band-gap PL might also be observable from small CNT ropes.

In summary, we have reported evidence for PL from small-diameter large band-gap core tubes in DWNT suspensions. Spectral features of the latter were best resolved if sodium- or ammonium-cholate was used as surfactant. Owing to small quantum yields the observed PL transients can be associated with the kinetics of nonradiative decay. The latter is found to correlate with tube diameter and the redshift of exciton transitions in different environments and suggests that tailoring of the tube environment may facilitate some control of PL-QYs in these systems.

Acknowledgment. H.U. acknowledges financial support by the Max Kade foundation. It is our pleasure to acknowledge support by G. Ertl, J. W. Tomm, and Th. Elsaesser.

References

- (1) Misewich, J. A.; Martel, R.; Avouris, P.; Tsang, J. C.; Heinze, S.; Tersoff, J. *Science* **2003**, *300*, 783–786.
- (2) Freitag, M.; Martin, Y.; Misewich, J. A.; Martel, R.; Avouris, P. H. *Nano Lett.* **2003**, *3*, 1067–1071.
- (3) Star, A.; Lu, Y.; Bradley, K.; Gruner, G. *Nano Lett.* **2004**, *4*, 1587–1591.
- (4) Ando, T. *J. Phys. Soc. Jpn.* **1997**, *66*, 1066–1073.
- (5) Perebeinos, V.; Tersoff, J.; Avouris, P. *Phys. Rev. Lett.* **2004**, *92*.
- (6) Hertel, T.; Moos, G. *Chem. Phys. Lett.* **2000**, *320*, 359–364.
- (7) Hertel, T.; Moos, G. *Phys. Rev. Lett.* **2000**, *84*, 5002–5005.
- (8) Hertel, T.; Fasel, R.; Moos, G. *Appl. Phys. A* **2002**, *75*, 449–465.
- (9) Ichida, M.; Hamanaka, Y.; Kataura, H.; Achiba, Y.; Nakamura, A. *Physica B–Condens. Matter* **2002**, *323*, 237–238.
- (10) Lauret, J. S.; Voisin, C.; Cassabois, G.; Delalande, C.; Roussignol, P.; Jost, O.; Capes, L. *Phys. Rev. Lett.* **2003**, *90*.
- (11) Moos, G.; Fasel, R.; Hertel, T. *J. Nanosci. Nanotechnol.* **2003**, *3*, 145–149.
- (12) Hagen, A.; Moos, G.; Talalaev, V.; Hertel, T. *Appl. Phys. A* **2004**, *78*, 1137–1145.
- (13) Kono, J.; Ostojic, G. N.; Zaric, S.; Strano, M. S.; Moore, V. C.; Shaver, J.; Hauge, R. H.; Smalley, R. E. *Appl. Phys. A* **2004**, *78*, 1093–1098.
- (14) Korovyanko, O. J.; Sheng, C. X.; Vardeny, Z. V.; Dalton, A. B.; Baughman, R. H. *Phys. Rev. Lett.* **2004**, *92*.
- (15) Ostojic, G. N.; Zaric, S.; Kono, J.; Strano, M. S.; Moore, V. C.; Hauge, R. H.; Smalley, R. E. *Phys. Rev. Lett.* **2004**, *92*.
- (16) Wang, F.; Dukovic, G.; Brus, L. E.; Heinz, T. F. *Phys. Rev. Lett.* **2004**, *92*.
- (17) Zaric, S.; Ostojic, G. N.; Kono, J.; Shaver, J.; Moore, V. C.; Strano, M. S.; Hauge, R. H.; Smalley, R. E.; Wei, X. *Science* **2004**, *304*, 1129–1131.
- (18) Colomer, J. F.; Henrard, L.; Flahaut, E.; Van Tendeloo, G.; Lucas, A. A.; Lambin, P. *Nano Lett.* **2003**, *3*, 685–689.
- (19) Flahaut, E.; Bacsá, R.; Peigney, A.; Laurent, C. *Chem. Commun.* **2003**, 1442–1443.
- (20) O’Connell, M. J.; Bachilo, S. M.; Huffman, C. B.; Moore, V. C.; Strano, M. S.; Haroz, E. H.; Rialon, K. L.; Boul, P. J.; Noon, W. H.; Kittrell, C.; Ma, J. P.; Hauge, R. H.; Weisman, R. B.; Smalley, R. E. *Science* **2002**, *297*, 593–596.
- (21) Lebedkin, S.; Arnold, K.; Hennrich, F.; Krupke, R.; Renker, B.; Kappes, M. M. *New J. Phys.* **2003**, *5*.
- (22) Moore, V. C.; Strano, M. S.; Haroz, E. H.; Hauge, R. H.; Smalley, R. E.; Schmidt, J.; Talmon, Y. *Nano Lett.* **2003**, *3*, 1379–1382.

NL050069A